An electrochemical dopamine sensor with a CMOS detection circuit

2008 J. Micromech. Microeng. 18 075028

(http://iopscience.iop.org/0960-1317/18/7/075028)

J. Micromech. Microeng. **18** (2008) 075028 (7pp) doi:10.1088/0960-1317/18/7/075028

An electrochemical dopamine sensor with a CMOS detection circuit

Feng-Lin Chan[1], Wen-Ying Chang[2], Li-Min Kuo[1], Chih-Heng Lin[2], Shi-Wei Wang[1], Yuh-Shyong Yang[2] and Michael S-C Lu[1,3]

[1] Institute of Electronics Engineering, National Tsing Hua University, Hsinchu, Taiwan, Republic of China
[2] Department of Biological Science and Technology, National Chiao Tung University, Hsinchu, Taiwan, Republic of China

E-mail: sclu@ee.nthu.edu.tw

Received 25 February 2008, in final form 28 April 2008
Published 13 June 2008
Online at stacks.iop.org/JMM/18/075028

Abstract
This paper presents the integration of interdigitated microelectrodes and a CMOS circuit for electrochemical sensing of the neurotransmitter dopamine. Gold electrodes with a gap of 3 μm are fabricated by the lift-off technique. The CMOS sensing circuit has a current gain of 10, an integrating capacitor of 4 pF, and a measured dynamic range of 60 dB. The applied reduction and oxidation potentials are determined by voltammetry at about -0.2 V and 0.6 V, respectively. The measured collection efficiency can reach up to 84%. The produced oxidation current with respect to dopamine concentration averages 0.44 nA μM^{-1}.

(Some figures in this article are in colour only in the electronic version)

1. Introduction

Parkinson's disease is a degenerative disease of the nervous system associated with trembling of the arms and legs, stiffness and rigidity of the muscles and slowness of movement. Until now, in humans, a deficiency of the neurotransmitter dopamine in the basal ganglia of the brain has been known well to play a critical role in Parkinson's disease. Dopamine acts like a brain chemical to transmit messages to parts of the brain for coordination of body movements. Medications or surgery can provide relief from the symptoms. Deep brain stimulation (DBS) is presently the most used surgical means of treatment. The surgery involves insertion of electrodes deep into the brain, usually on the subthalamic nucleus in a Parkinson's patient. Low-voltage electrical pulses transmitted to the brain are intended to block the abnormal firing of neurons as caused by a lack of dopamine. Gene therapy and implantation of stem cells are among the methods under evaluation. The long-term goal of this research is to develop a miniaturized, implantable dopamine sensor capable of providing real-time and localized detection of dopamine concentration in a patient's brain, allowing convenient monitoring of a patient's progress after the surgery. Integration of the associated sensing circuit can reduce the device size and simplify the data acquisition process. The basic idea has been practiced in the early work where microelectrodes were used to monitor the capabilities of cell transplants to release monoamine [1]. Wightman *et al* [2] also implanted stimulating electrodes in the vicinity of the axons of dopamine neurons and used electrodes fabricated from carbon fibers to detect the dopamine secretion.

Interdigitated microelectrodes have been widely adopted to study electrochemical reaction of various electroactive species for quantitative analysis. The main advantage, as the width and gap of the microelectrodes are reduced by microfabrication, is the achieved high sensitivity due to the enhanced redox current and redox cycles. The improved signal-to-noise ratio has made them suitable for use as electrochemical detectors in high-performance liquid chromatography (HPLC) [3] and electrophoresis [4]. Interdigitated microelectrodes can be used as enzyme immunoassays for rapid testing of a variety of clinical analytes [5–8]. For example, Honda *et al* [7] reported the immunoassay of alpha-fetoprotein (AFP, a clinical diagnostic protein marker) for hepatic carcinoma.

Apart from using interdigitated microelectrodes that have been studied mostly by chemists, this work also aims at integrating the detection circuit to realize a fully functional

[3] Address for correspondence: Department of Electrical Engineering, National Tsing Hua University, 101 Sec 2 Kuang-Fu Road, Hsinchu 30013, Taiwan, Republic of China.

sensor [9], such as the DNA sensor reported by Schienle *et al* [10]. The circuit has to convert the produced redox current to a sensed voltage, and provide the bias for electrochemical reaction to take place; for example, the switched-capacitor circuit by Stanaćević [11] reported a sensing resolution of 100 fA and detected a sensed current of 100 pA at a dopamine concentration of 5 μM. This work shows the produced current is enhanced by the microelectrodes, and the measured value is in the order of nA with respect to dopamine concentration in the μM range.

2. Microelectrodes

Interdigitated microelectrodes with a narrow linewidth, especially in the micrometer range, provide the capability for more sensitive detection than the conventional electrodes, as the chemical products produced at one side of the electrodes can be readily collected at the other side of adjacent electrodes and regenerated to the original states. Thus the anodic and cathodic currents increase due to the phenomenon of fast redox recycling. The complete microelectrode setup for producing an electrochemical reaction generally consists of two interdigitated working electrodes, one counter electrode and one reference electrode. As a common practice, an external Ag/AgCl reference electrode will be immersed into the solution for our experiments. The other electrodes can be made of conductive thin films, particularly gold [12, 13], platinum [14, 15], and carbon [16–19]. Carbon electrodes have a wider potential range than those of metal films during electroanalysis and can produce a lower baseline current without redox species [18]. Conductive carbon electrodes with good adhesion are relatively difficult to produce in a conventional sputtering system, and they are usually deposited by pyrolysis at about 1000 °C. As the processing technology advances, Fiaccabrino *et al* [19] have reported good-quality carbon thin films produced at a low temperature in a magnetron sputtering system.

Gold was used in this work as the electrode material. Low-stress silicon dioxide was first deposited on a p-type silicon substrate by low-pressure chemical vapor deposition. After optical lithography and metal evaporation (50 nm Au and 5 nm Cr for adhesion), the microelectrodes were fabricated by the lift-off technique.

3. Electrochemical reaction

Dopamine can be oxidized at the anode by producing two electrons and dopamine ortho-quinone, and reduced back at the adjacent cathode when a proper reduction potential is given. The relationship between the produced redox current and the sample concentration has to be understood first before designing the detection circuit. The topic was first studied using semi-empirical equations by Sanderson [20], and later the diffusion-limited current under the steady state was derived by Aoki *et al* [21] as given by

$$I = lmnFDc\{0.637 \ln[2.55(1 + w/g)] - 0.19[g/(w + g)]^2\} \quad (1)$$

where l and m are the length and the pair of the microelectrodes, n is the number of electrons, F is the Faraday constant ($F = 96487$ C mol^{-1}), D is the diffusion coefficient, c is the concentration, w is the microelectrode width and g is the gap between electrodes. The equation is obtained by solving the two-dimensional diffusion equation using Schwartz–Christoffel transformation, and can be used for w and g in the range between 2 and 10 μm as verified by experiments. For electrodes with larger dimensions the electrochemical reaction may have fluctuations due to natural convection during the long electrolysis, leading to less reproducibility [21]. For example, the produced current is 1.14 nA for a dopamine concentration of 2 μM by using the following parameters: $l = 150$ μm, $m = 30$, $g = w = 3$ μm and $D = 6.65 \times 10^{-6}$ cm^2 s^{-1} [22, 23]. The sensitivity is 0.57 nA μM^{-1}. The minimum linewidth of the microelectrodes in this work is 3 μm as limited by the lithographic process.

The ratio of the produced cathodic current to the anodic current is defined as the collection efficiency [24], which depends on the electrode dimensions and the flow rate, if a flow-cell setup is available. High collection efficiency can be obtained when the gap between electrodes is in the same order as the diffusion layer thickness [21]. Paeschke *et al* [25] reported microelectrodes with a sub-μm gap which is in the same order as the diffusion layer thickness for improving the collection efficiency. 3D comb electrodes have also been used to enhance trapping of the redox species inside the comb structures [7]. The number of redox cycles increases as the gap decreases, as it is closely related to the collection efficiency as given by [13]

$$N_c = \frac{1}{1 - CE^2} \quad (2)$$

where N_c is the redox cycle number and CE is the collection efficiency. The difference in species diffusion constants has negligible effect on the collection efficiency and redox cycle. The collection efficiency decreases as the flow rate increases because the diffusion of redox species from the bulk solution is more dominant than that between the electrodes. Both the signal-to-noise ratio and the dynamic range can be increased with a high collection efficiency or a large number of redox cycles.

4. Sensing circuit design

The CMOS sensing circuit as shown in figure 1(a) is designed and fabricated by using the TSMC 0.35 μm CMOS process. All transistors are operated at the standard 3.3 V. The anode (generator) electrode is connected to the circuit and its bias is provided through the virtual ground of an operational amplifier as shown in figure 1(b). The gate of the M1 transistor provides isolation between the op-amp and the sensing node; in addition, the potential at the sensing node is regulated by the use of a large external capacitor C_1 in the order of nF. The amplifier is a conventional two-stage op-amp design with p-type input transistors. It has an open-loop gain of 67 dB, a unity-gain frequency of 32 MHz and a phase margin of 70° by simulation (output load = 20 pF and 1 MΩ). The final

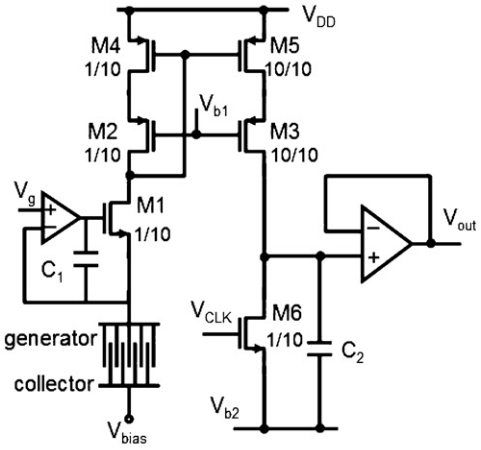

(*a*)

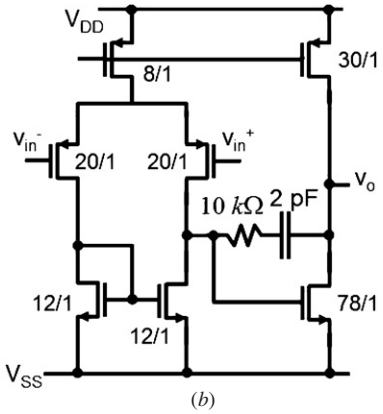

(*b*)

Figure 1. (*a*) Schematic of the CMOS circuit for dopamine detection. (*b*) Schematic of the op-amp design as shown in (*a*). The labeled transistor width and length are in μm.

output voltage is produced through a buffer circuit which is also made of the same operational amplifier. The produced oxidation current at the anode is amplified by the wide-swing cascade current mirror (M2 to M5) with a current gain of 10. The amplified current is then converted to a voltage by the use of an integrating capacitor C_2 with a value of 4 pF. An external clock signal V_{CLK} constantly resets the output and controls the integration time through the M6 transistor. The buffer input is reset to the potential provided by the voltage V_{b2}. Simulation results show the circuit can provide a constant current gain in the range between 0.2 nA and 0.4 μA, equivalent to a dynamic range of 66 dB. By removing the input current source of the current mirror in simulation, an input-referred leakage current of 6.4 pA produces a 0.8 V output in a 50 ms span. The total circuit size is 370 μm $\times$ 280 μm. For an input current of 1 nA, the current mirror and the op-amp consume 36 nW and 0.9 mW, respectively.

5. Experiment

Figure 2(*a*) shows the fabricated interdigitated microelectrodes after lift-off. The microelectrode die and the CMOS die were placed on a small PC board and connected through wirebond; in addition, the CMOS die was covered by epoxy as shown in figure 2(*b*). The electrical performance of the sensor should

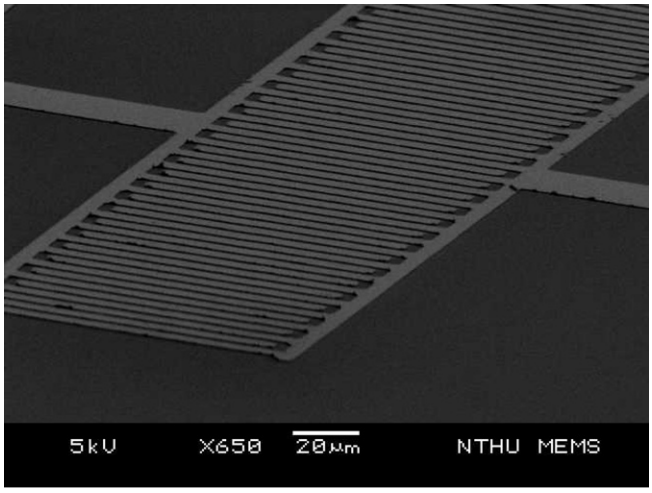

(*a*)

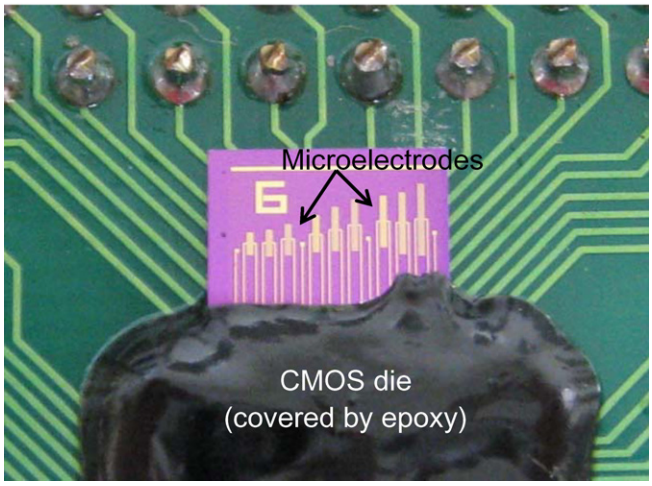

(*b*)

Figure 2. (*a*) Scanning electron micrograph of the fabricated microelectrodes. (*b*) Micrograph of the microelectrode die and the CMOS die on a small printed circuit board.

not be affected by the hybrid integration as the electrode bias is fixed by the op-amp such that the bond-pad capacitor does not integrate the produced current. Output waveforms were measured at input current values from 10 pA to 1 μA as provided by a sourcemeter. Figure 3(*a*) shows the waveform for the 100 pA case which increases from 0.5 V ($V_{b2} = 0.5$ V) to 2 V in 5 ms. Figure 3(*b*) depicts the current gains for all cases obtained by experiment and simulation. The measured gain curve deviates from the desired gain of 10 at tenths of pA and hundreds of nA. The measured dynamic range is about 60 dB, 6 dB less than the simulated value. The inaccuracy of the simulated current gain for low current values can be explained by taking the simulated leakage current of 6.4 pA into account. The measured leakage is about twice the simulated value to produce a larger deviation in the measured current gain. In the case where a constant gain is required for an input current up to μA, the bias voltage V_{b1} of the circuit can be lowered such that the transistors in the current mirror can operate in the saturation region.

The electrochemical experiment was performed at room temperature (25 °C) and atmospheric pressure.

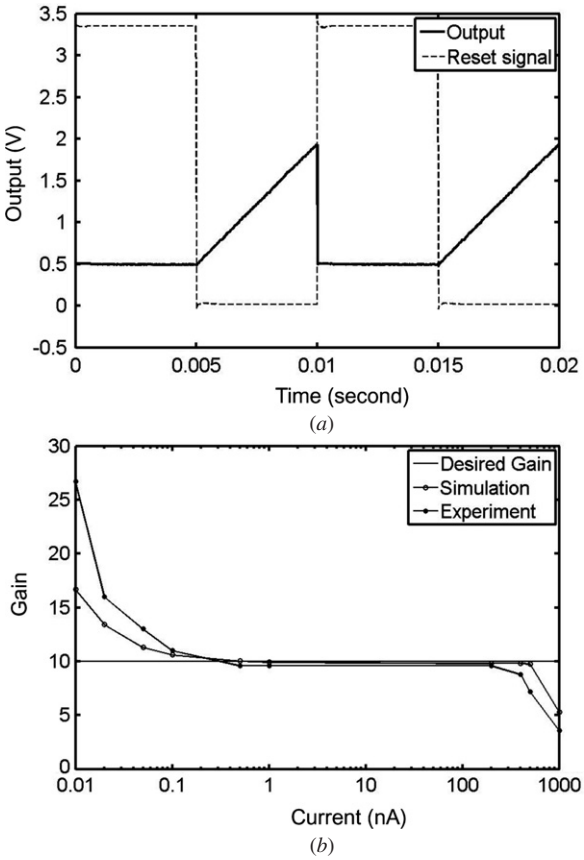

Figure 3. (*a*) Measured circuit output waveform at an input current value of 100 pA. (*b*) The gain of the current mirror at different input current values.

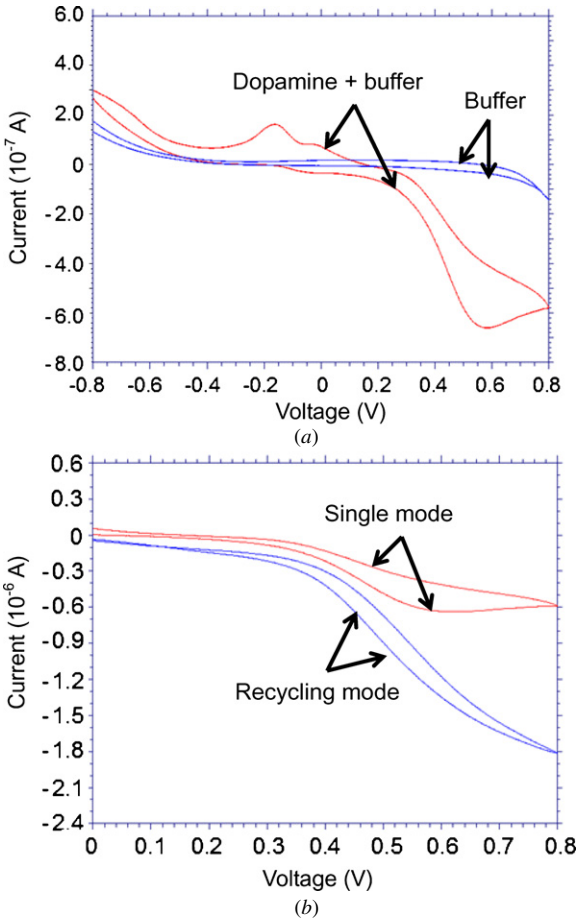

Figure 4. (*a*) Measured cyclic voltammograms of 1 mM dopamine and 20 μM buffer. (*b*) Measured cyclic voltammograms of 1 mM dopamine by the single mode and the recycling mode.

Cyclic voltammetry was performed using the fabricated microelectrodes to identify the respective oxidation and reduction potentials for dopamine (Sigma-Aldrich, USA) in phosphate buffer solution (pH = 8.1, J. T. Baker, USA). In the single-mode operation where only one set of the working electrodes ($l = 150$ μm, $g = 3$ μm and 35 microbands) was used, the molecules adjacent to the electrode were oxidized or reduced in the cyclic voltammetry, depending on the voltage value. Figure 4(*a*) shows the measured result of 1 mM dopamine by using an electrochemical workstation (Model 701B, CH Instruments, Austin, TX) at a scan rate of 50 mV s^{-1}. The curves show the current values become positive and negative when reduction and oxidation take place, respectively. One peak occurs at about -0.15 V and the other at about 0.5 V, both with respect to the Ag/AgCl reference electrode. The values near the two peaks can be used as the reduction and oxidation potentials. Electroactive functional groups presented on the electrode surface can also be oxidized or reduced, producing an additional background current that limits the minimum detectable concentration of the desired target. The other curve in the figure shows the electrochemical reaction of the buffer solution of 20 μM. Next in figure 4(*b*) we show the measured current values from both the single-mode and the recycling-mode operations. In the recycling mode, the cathode was fixed at a reduction potential of -0.5 V and the anode potential was swept from 0 V to 0.8 V then back to 0 V at a scan rate of 50 mV s^{-1}. The steady-state current in the recycling mode is about three times of that in the single mode, close to the value reported in [26]. Niwa concluded that the current in the recycling mode should be almost the same as that in the single mode when the analyte is injected at a high flow rate; however the current in single mode decreases at a low flow rate while the current in the recycling mode keeps almost unchanged. There was no flow-cell setup in our experiment. The flow rate was therefore zero.

For the following experiments, the anode was held at 0.6 V and the cathode at -0.2 V with respect to the Ag/AgCl reference electrode. Dopamine solutions of concentrations from 2 μM to 30 μM (pH values between 6.54 and 6.81) were separately added to microelectrodes ($l = 150$ μm, $g = 3$ μm, $w = 3$ μm and 30 pairs) and the produced reduction and oxidation currents were recorded by the electrochemical workstation. Figure 5 shows that after dopamine was added, it took about a few hundred seconds for the responses to reach steady states. The long reaction time can be significantly reduced to few tenths of seconds by establishing a flow-cell setup that can confine the solution in a small cell volume at a fixed flow rate [26]. The measured reduction and oxidation current values with respect to the dopamine concentration are plotted in figure 6 after subtracting the background current values, which are 0.43 nA and 1.5 nA for oxidation and

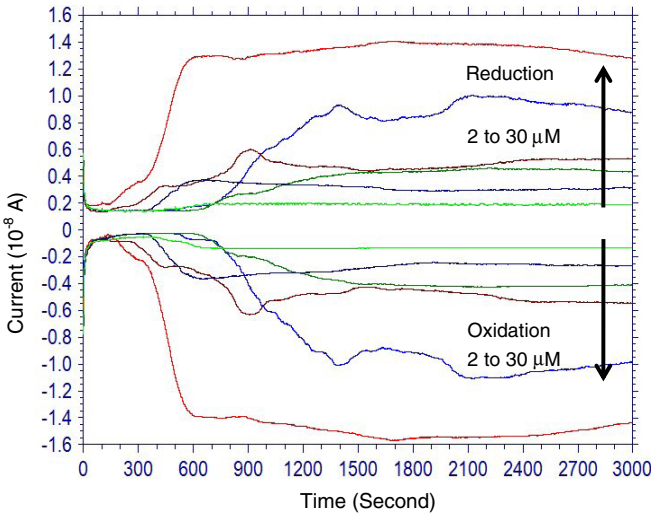

Figure 5. Measured current values with respect to time for dopamine concentrations from 2 μM to 30 μM.

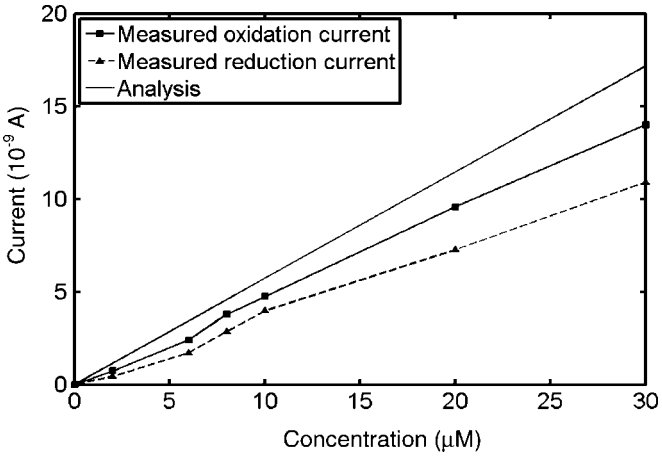

Figure 6. Relationship of the measured steady-state oxidation and reduction currents with respect to the dopamine concentration.

reduction, respectively. The produced oxidation current with respect to dopamine concentration averages 0.44 nA μM^{-1} as shown by the curve. The collection efficiency can reach up to 84% for dopamine concentration at 10 μM, with an average value of 73% based on all measured data. The figure also indicates the measured oxidation current values are lower than the calculated ones from equation (1) by an average of 22%. The deviation can be partly attributed to the reproducibility of the experiment that is affected by electrode cleanness, roughness and chemical conditions, etc.

The CMOS detection circuit and the microelectrodes were connected and biased as shown in figure 7 to perform the electrochemical detection. An electrometer (Keithley 6514) was connected in series with the generator electrode to measure the oxidation current, which was amplified and converted to a voltage waveform by the CMOS circuit. Phosphate buffer solution (99.8 μL and 20 μM) was first added to the microelectrodes. Then at the instants of 200 and 2200 s, 1 mM dopamine solutions of 0.2 μL were injected respectively to

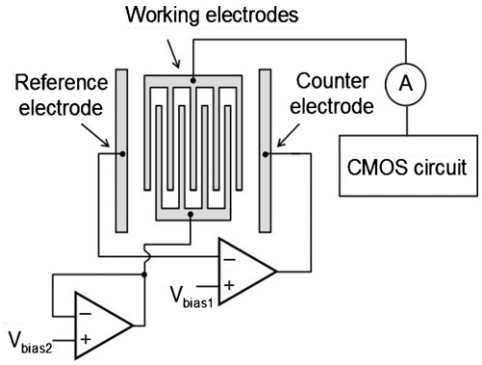

Figure 7. Experimental setup of microelectrodes and CMOS circuit for electrochemical sensing.

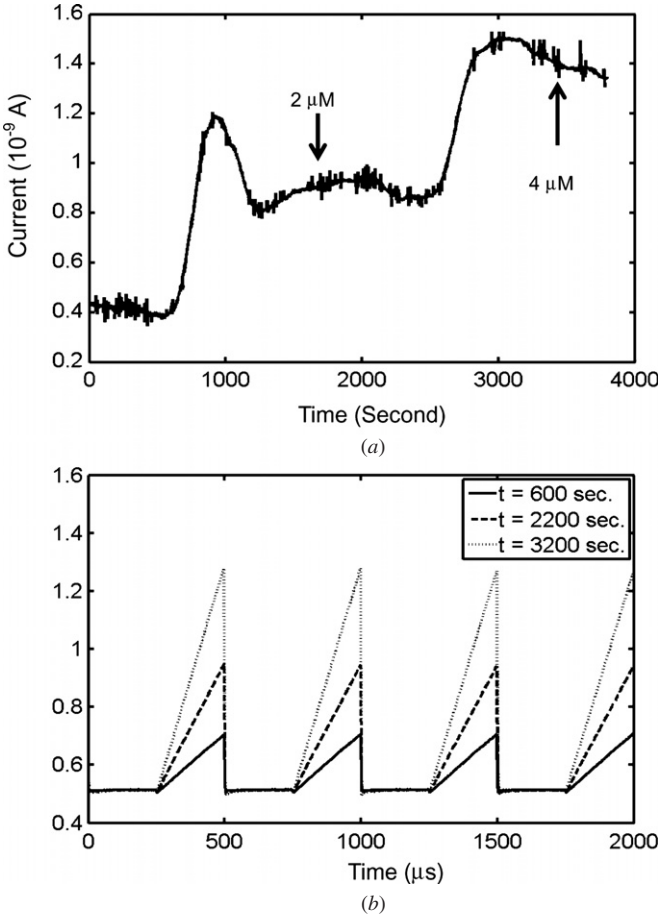

Figure 8. (*a*) Measured current values for dopamine concentrations of 2 μM and 4 μM. (*b*) Measured output waveforms from the CMOS sensing circuit at instants of 600, 2200 and 3200 s, respectively, as the current value increases.

produce equivalent dopamine concentrations of 2 μM and 4 μM. Figure 8(*a*) depicts the recorded current values with a background value of about 0.4 nA. The corresponding output waveforms from the CMOS circuit at different time instants as in figure 8(*a*) were measured as plotted in figure 8(*b*). By using microelectrodes, the sensitivity of produced current with respect to dopamine concentration is about 70 times higher than the value (20 pA μM^{-1}) reported in [11].

6. Discussion and conclusion

This work presents the use of interdigitated gold electrodes with CMOS circuit for electrochemical detection of dopamine. Monolithic integration by post-CMOS processing can be achieved when a CMOS wafer is available such that lithography and surface planarization can be performed for electrode fabrication. Cyclic voltammetry has been performed to find the respective oxidation and reduction potentials for dopamine. The maximum collection efficiency can reach up to 84% at zero flow rate. The measured current values increase quite linearly with respect to the dopamine concentration, and differ from the calculated values by an average of 22%. A flow-cell setup with flow-rate control can be used to improve the long diffusion time of the redox reaction by one to two orders of magnitude.

The minimum detectable concentration is currently in the range of μM as limited by the background current of about 500 pA. This current is largely contributed by the sensing interface consisting of the electrode and the analyte, with a small portion of 10–15 pA from the leakage of the CMOS detection circuit. Detection down to the nM level could be achieved by using carbon electrodes as reported in prior work, and the corresponding produced current would likely be in the pA range. In that case, the current circuit topology may need to be modified since some of the transistors in the current mirrors have to operate deep into the sub-threshold region and the leakage current can become an issue. A less advanced CMOS process is desired for reducing the transistor leakage. The switched-capacitor circuit [11] could be one of the circuit topologies to consider. The overall consumed power can be further reduced by using a low-power op-amp design. For future *in vivo* measurement in a brain, the use of perfluorinated ion-exchange membranes can lead to improved microelectrodes in terms of selectivity and sensitivity. For example, nafion-coated electrodes [27] can be used to improve selectivity of dopamine with respect to other electroactive species, such as ascorbate and dihydroxyphenylacetic acid (a metabolite of dopamine).

Acknowledgments

The authors would like to thank the National Tsing Hua University and the National Science Council, Taiwan, Republic of China, for support of this research effort. We are also grateful to the National Chip Implementation Center for support of chip fabrication, and the National Center for High-Performance Computing for support of simulation software.

References

[1] Rose G, Gerhardt G, Stromberg I, Olson L and Hoffer B 1985 Monoamine release from dopamine-depleted rat caudate-nucleus reinnervated by substantia nigra transplants—an *in-vivo* electrochemical study *Brain Res.* **341** 92–100

[2] Wightman R M, May L J and Michael A C 1988 Detection of dopamine dynamics in the brain *Anal. Chem.* **60** 769A–79A

[3] Tabei H, Takahashi M, Hoshino S, Niwa O and Horiuchi T 1994 Subfemtomole detection of catecholamine with interdigitated array carbon microelectrodes in HPLC *Anal. Chem.* **66** 3500–2

[4] Wallingford R A and Ewing A G 1988 Capillary zone electrophoresis with electrochemical detection in 12.7 mm diameter columns *Anal. Chem.* **60** 1972–5

[5] Niwa O, Xu Y, Halsall H B and Heineman W R 1993 Small-volume voltammetric detection of 4-aminophenol with interdigitated array electrodes and its application to electrochemical enzyme immunoassay *Anal. Chem.* **65** 1559–63

[6] Wollenberger U, Paeschke M and Hintsche R 1994 Interdigitated array microelectrodes for the determination of enzyme activities *Analyst* **119** 1245–9

[7] Honda N, Inaba M, Katagiri T, Shoji S, Sato H, Homma T, Osaka T, Saito M, Mizuno J and Wada Y 2005 Highly effciency electrochemical immuno sensors using 3D comb electrode *Biosens. Bioelectron.* **20** 2306–9

[8] Diaz-Gonzalez M, Gonzalez-Garcia M B and Costa-Garcia A 2005 Recent advances in electrochemical enzyme immunoassay *Electroanalysis* **17** 1901–18

[9] Zhan F L, Kuo L M, Chang W Y, Wang S W, Lin C H, Yang Y S and Lu M S C 2007 An electrochemical dopamine sensor with CMOS detection circuit *IEEE Int. Conf. Sensor (Atlanta, USA)* pp 1448–51

[10] Schienle M, Paulus C, Frey A, Hofmann F, Holzapfl B, Schindler-Bauer P and Thewes R 2004 A fully electronic DNA sensor with 128 positions and in-pixel A/D conversion *IEEE J. Solid-State Circuit* **39** 2438–45

[11] Stanaćević M, Murari K, Rege A, Cauwenberghs G and Thakor N 2007 VLSI potentiostat array with oversampling gain modulation for wide-range neurotransmitter sensing *IEEE Trans. Biomed. Circuits Syst.* **12** 63–72

[12] Niwa O, Morita M and Tabei H 1989 Fabrication and characteristics of vertically separated interdigitated array electrodes *J. Electroanal. Chem.* **267** 291–7

[13] Niwa O, Morita M and Tabei H 1990 Electrochemical behavior of reversible redox species at interdigitated array electrodes with different geometries—consideration of redox cycling and collection efficiency *Anal. Chem.* **62** 447–52

[14] Chidsey C E, Feldman B J, Lundgren C and Murray R W 1986 Micrometer-spaced platinum interdigitated array electrode—fabrication, theory and initial use *Anal. Chem.* **58** 601–7

[15] Feldman B J and Murray R W 1986 Measurement of electron-diffusion coefficients through Prussian blue electroactive films electrodeposited on interdigitated array platinum electrodes *Anal. Chem.* **58** 2844–7

[16] Aoki K and Tanaka M 1989 Time-dependence of diffusion-controlled currents of a soluble redox couple at interdigitated microarray electrodes *J. Electroanal. Chem.* **266** 11–20

[17] Tabei H, Morita M, Niwa O and Horiuchi T 1992 Fabrication and electrochemical features of new carbon based interdigitated array microelectrodes *J. Electroanal. Chem.* **334** 25–33

[18] Niwa O and Tabei H 1994 Voltammetric measurements of reversible and quasi-reversible redox species using carbon film based interdigitated array microelectrodes *Anal. Chem.* **66** 285–9

[19] Faiccabrino G C, Tang X M, Skinner N, de Rooij N F and Koudelka-Hep M 1996 Interdigitated microelectrode arrays based on sputtered carbon thin-films *Sensors Actuators* B **35–36** 247–54

[20] Sanderson D G and Anderson L B 1985 Fliar electrodes—steady-state currents and spectroelectrochemistry at twin interdigitated electrodes *Anal. Chem.* **57** 2388–93

[21] Aoki K, Morita M, Niwa O and Tabei H 1988 Quantitative analysis of reversible diffusion-controlled currents of redox soluable species at interdigitated array electrodes under steady-state conditions *J. Electroanal. Chem.* **256** 269–82

[22] Hsieh S and Jorgenson J W 1996 Preparation and evaluation of slurry-packed liquid chromatography microcolumns with inner diameters from 12 to 33 mm *Anal. Chem.* **68** 1212–7

[23] Williams K R, Adhyaru B, German I and Russell T 2002 Determination of a diffusion coefficient by capillary electrophoresis—an experiment for the physical and biophysical chemistry laboratories *J. Chem. Educ.* **79** 1475–6

[24] Shea T V and Bard A J 1987 Digital simulation of homogeneous chemical reaction coupled to heterogeneous electron transfer and applications at platinum mica platinum ultra-micro-band electrodes *Anal. Chem.* **59** 2101–11

[25] Paeschke M, Wollenberger U, Lisec T, Schnakenberg U and Hintsche R 1995 Highly sensitive electrochemical microsensors using submicrometer electrode arrays *Sensors Actuators* B **26–27** 394–7

[26] Kurita R, Tabei H, Liu Z, Horiuchi T and Niwa O 2000 Fabrication and electrochemical properties of an interdigitated array electrode in a microfabricated wall-jet cell *Sensors Actuators* B **71** 82–9

[27] Gerhardt G A, Oke A F, Nagy G, Moghaddam B and Adams R M 1984 *Brain Res.* **290** 390–5